

Universal logarithmic corrections to entanglement entropies in two dimensions with spontaneously broken continuous symmetries

David J. Luitz, Xavier Plat, Fabien Alet, and Nicolas Laflorencie

Laboratoire de Physique Théorique, IRSAMC, Université de Toulouse, CNRS, 31062 Toulouse, France

(Dated: April 4, 2024)

We explore the Rényi entanglement entropies of a one-dimensional (line) subsystem of length L embedded in two-dimensional $L \times L$ square lattice for quantum spin models whose ground-state breaks a continuous symmetry in the thermodynamic limit. Using quantum Monte Carlo simulations, we first study the $J_1 - J_2$ Heisenberg model with antiferromagnetic nearest-neighbor $J_1 > 0$ and ferromagnetic second-neighbor couplings $J_2 \leq 0$. The signature of $SU(2)$ symmetry breaking on finite size systems, ranging from $L = 4$ up to $L = 40$ clearly appears as a universal additive logarithmic correction to the Rényi entanglement entropies: $l_q \ln L$ with $l_q \simeq 1$, independent of the Rényi index and values of J_2 . We confirm this result using a high precision spin-wave analysis (with restored spin rotational symmetry) on finite lattices up to $10^5 \times 10^5$ sites, allowing to explore further non-universal finite size corrections and study in addition the case of $U(1)$ symmetry breaking. Our results fully agree with the prediction $l_q = n_G/2$ where n_G is the number of Goldstone modes, by Metlitski and Grover [arXiv:1112.5166].

I. INTRODUCTION

Entanglement entropy (EE) is now well recognized as a very powerful tool to diagnose various quantum states of matter^{1,2}. For interacting quantum systems in dimension $D \geq 2$, the ground-state EE of a given spatial partition A embedded in a larger system scales with the perimeter ℓ_A of A , following the so-called area-law^{3,4} for any Rényi index $q > 0$

$$S_q = \frac{1}{1-q} \ln \left(\text{Tr} [\hat{\rho}_A]^q \right) = a_q \ell_A + \dots \quad (1.1)$$

where $\hat{\rho}_A$ is the reduced density matrix of the subsystem A . While the leading part $a_q \ell_A$ is not expected to reflect the universality of the phase, sub-leading terms (the ellipsis in Eq. (1.1) above) may encode it, as first discovered for topological order^{5,6}. For systems which exhibit a true long-range order in the ground-state with a continuous symmetry breaking in the thermodynamic limit, the EE of a subsystem has been predicted⁷ to exhibit a universal additive logarithmic correction to the area law term, with a prefactor in dimension $D = 2$ controlled by the number of Goldstone modes n_G associated to the broken symmetry:

$$S_q = a_q \ell_A + \frac{n_G}{2} \ln \ell_A + \dots \quad (1.2)$$

In such finite systems (with $N = L \times L$ sites), there are two types of excitations: the Anderson tower of states (TOS)⁸ with an energy scaling as $1/L^2$ and n_G Goldstone modes (SW for quantum magnets) with a linear dispersion $\sim 1/L$, both being key contributions for the expected logarithmic corrections in Eq. (1.2)⁷. As first detected using a modified spin-wave (SW) approach for the $SU(2)$ symmetric Heisenberg antiferromagnet on a square lattice⁹, subsequent quantum Monte Carlo (QMC) calculations^{10–12} have also been able to capture additive logarithmic corrections, while estimates of the prefactor did

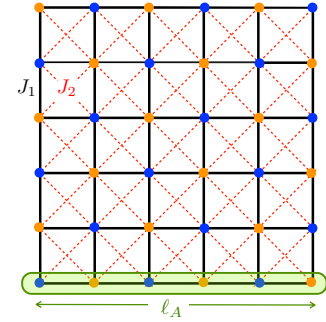


Figure 1. Schematic picture for the $J_1 - J_2$ square lattice. The line shaped subsystem A of length ℓ_A is shown in green.

not agree with the prediction. Also, the expected factor of two between the logarithmic terms for $SU(2)$ and $U(1)$ was not clearly observed¹¹. The possible reasons for such discrepancies are temperature and/or statistical effects, as well as the importance of further finite-size corrections (beyond the log term) which might be hard to capture with QMC simulations on finite-size systems. Also one has to carefully subtract contributions to logarithmic corrections to S_q from corners if present in the subsystem geometry^{10,12}: these contributions are usually numerically small and their estimates from QMC simulations are suffering from the above mentioned difficulties.

Very recently, Kulchytskyy *et al.* used an improved estimator for S_2 (for a half-torus subsystem) with QMC simulations of the spin- $\frac{1}{2}$ XY model on the square lattice¹³ which allowed them to get a quite precise estimate for the prefactor of the log correction $\simeq 0.5$, fully consistent with $n_G = 1$ Goldstone boson associated to the breaking of $U(1)$ symmetry. Nevertheless, to the best of our knowledge there is no numerical study demonstrating the universality of Eq. (1.2), such as its independence on the Rényi index q , details of microscopic Hamiltonian or type of continuous symmetry breaking.

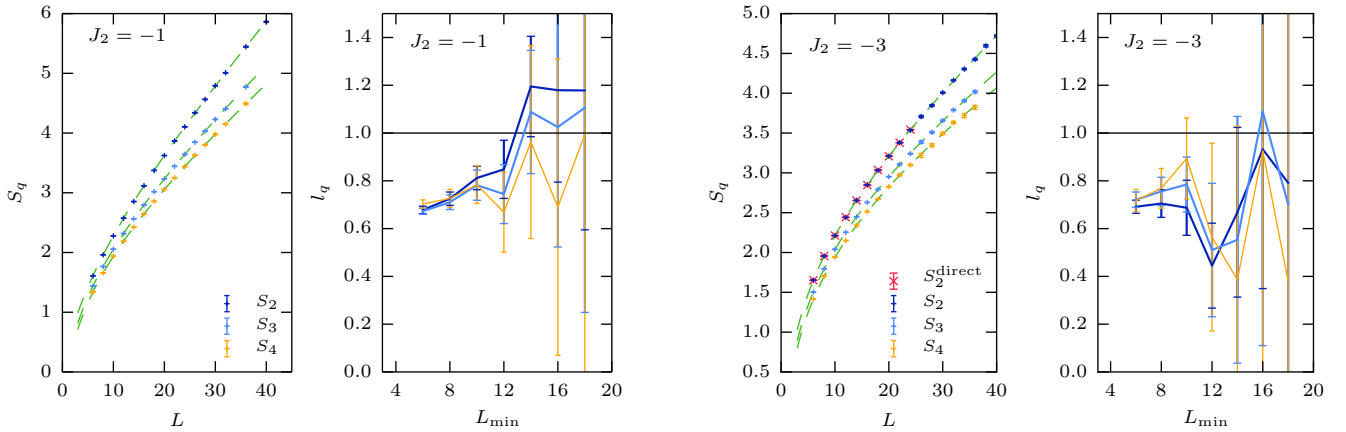


Figure 2. (Color online) QMC results for the entanglement Rényi entropies of the $J_1 - J_2$ Heisenberg model for $J_2 = -1$ (left two panels) and $J_2 = -3$ (right two panels). We show the prefactor of the logarithmic scaling term obtained by fits to the form $S_q = a_q L + l_q \ln L + b_q + c_q/L$ over fit ranges $[L_{\min}, L_{\max}]$ as a function of L_{\min} , with $L_{\max} = 40$ for $q = 2$ and $L_{\max} = 36$ for $q = 3, 4$. Our results are consistent with $l_q = 1$ independent of J_2 and q . For $J_2 = -3$, we also show the EE S_2^{direct} obtained by a direct mixed ensemble calculation using the method of Ref. 11.

In this paper, we aim at going further to test the prediction Eq. (1.2) for various values of q and for two quantum spin models having different symmetries, using a one-dimensional ring of length $\ell_A = L$ as subsystem A (see Fig. 1) embedded in a $L \times L$ torus. This is the simplest possible corner-free bipartition scaling with L where the universal logarithmic correction proportional to the number of Goldstone modes should be present.

We explore the Rényi EEs S_q for such a subsystem using two techniques: exact QMC simulations of S_q with $q = 2, 3, 4$ (Sec. II), and a semi-classical SW theory for finite size systems^{14,15} where spin rotational invariance is restored such that both TOS and Goldstone modes are included (Sec. III). The choice of a line subsystem is advantageous for these two techniques: in QMC, we use the improved estimator introduced in Ref. 16, which is particularly efficient when subsystem volume is as small as possible (it is in fact minimal for the line subsystem), while the SW calculations are particularly simplified by full translation symmetry of the line subsystem, allowing for an analytical understanding of the $\frac{n_G}{2} \ln L$ term of Eq. (1.2).

II. QUANTUM MONTE CARLO RESULTS

For our quantum Monte Carlo calculations, we consider the spin-1/2 $J_1 - J_2$ antiferromagnet defined on a bipartite $L \times L$ square lattice by the following Hamiltonian

$$\mathcal{H}_{J_1-J_2} = J_1 \sum_{\langle ij \rangle} \vec{S}_i \cdot \vec{S}_j + J_2 \sum_{\langle\langle ij \rangle\rangle} \vec{S}_i \cdot \vec{S}_j, \quad (2.1)$$

where \vec{S} are spin- $\frac{1}{2}$ operators, interactions act between nearest neighbors $\langle ij \rangle$ and second nearest neighbours

$\langle\langle ij \rangle\rangle$ along the diagonals of the square lattice (see Fig. 1). For this work, we consider antiferromagnetic nearest neighbors interactions $J_1 > 0$ and *ferromagnetic* second neighbors interactions $J_2 < 0$, for which it is known that the ground-state exhibits antiferromagnetic long-range order, thus breaking $SU(2)$ symmetry associated with two Goldstone modes (independent of $J_2 < 0$). The motivation for adding the second neighbors interaction J_2 is to check the universality of the results with respect to microscopical variations of the Hamiltonian (different values of J_2) without changing the nature of the ground-state and of the low-lying excitations. Additionally, as $|J_2|$ is increased, the antiferromagnetic long-range order is enhanced (*i.e.* larger values of the order parameter), and we therefore expect lower EEs as we get closer to a classical Heisenberg antiferromagnet.

We perform extensive QMC simulations of this model for two different values of J_2 using the stochastic series expansion (SSE) algorithm^{17,18}. We compute the Rényi EE S_q for $q = 2, 3, 4$ using a recently introduced decomposition¹⁶ that benefits from subsystem symmetries. This method is particularly useful when the surface of the subsystem scales as its volume, *i.e.* if the subsystem volume is minimal without introducing geometrical effects, such as corners. In this sense, this method is optimal for the line shaped subsystem in Fig. 1.

Our simulations are performed in the finite temperature formulation of the SSE at low enough temperatures in order to capture only ground-state physics. While the finite size gap of the tower of states scales as the inverse of the total number of spins $N = L \times L$ in the system, one would expect that it is necessary to scale the inverse temperature β linearly in N . For the system sizes we studied (up to $L = 40$), we find however that the results for the EE of simulations at inverse temperatures

$\beta = 8L$ and $\beta = 4L$ agree within errorbars: we therefore performed all calculations at inverse temperatures higher than $\beta = 4L$. Fig. 2 shows the QMC result of the line EEs as a function of system size for different Rényi indices and two values of J_2 . For $J_2 = -3$ and $q = 2$, we also perform an independent set of QMC simulations in an extended ensemble where EE is directly computed from the ratio of partition functions¹¹. We obtain a perfect agreement between the two methods. Note, that the decomposition of the EE as described in Ref. 16 allows us to access larger system sizes (in particular for higher Rényi indices) with very high precision.

We fit our results for the line EEs to the scaling ansatz

$$S_q = a_q \ell + l_q \ln \ell + b_q + c_q/L \quad (2.2)$$

to infer if the prefactor of the logarithmic term is indeed $l_q = n_G/2$ ($= 1$ for the ground-state of the model Eq. 2.1). We systematically reduce the fitting range $[L_{\min}, L_{\max}]$ of included system sizes, always including the largest systems with $L_{\max} \sim 40$ and studying the best fit value of l_q as a function of L_{\min} as shown in the right panels of Fig. 2. Note that the errorbars stem from a careful bootstrap study of the stability of the fit introducing gaussian resampling of the data and perturbations of the initial parameters. We have studied the statistical behavior of the fit-data distance quantified by χ^2 and find that the qualities¹⁹ Q of the best fit are already very good (around 0.7...0.9) using the scaling ansatz from equation (2.2). Hence, the quality of our data does not allow for an inclusion of higher order terms (which could result in overfitting statistical noise).

While the log term is clearly present as nicely visible in the concavity of $S_q(L)$, we found it difficult to get a very precise estimate for the prefactor l_q in the thermodynamic limit. What is clear however is that whereas the area law term does depend on the Rényi index q and J_2 , there is apparently no q -dependence for l_q . Taking into account the largest L_{\min} , we can estimate that $l_q = 1.0(3)$, fully compatible with the prediction $l_q = 1$, albeit with admittedly large error bars. In order to reach much larger systems (which would be helpful in studying the convergence of l_q with L_{\min}), we now consider a SW calculation of EE for the same setup of a line subsystem.

III. SPIN-WAVE THEORY

Modified SW theory for finite size systems^{14,15} has been shown to be very useful for computing EEs of the square lattice Heisenberg antiferromagnet in Ref. 9. The crucial point is to artificially restore the spin rotational invariance in order to mimic the symmetric ground-state of a finite size system. For this, a size-dependent regularizing external field h^* is imposed to the system such that the SW-corrected order parameter is identically zero.

We study the $J_1 - J_2$ Heisenberg antiferromagnet Eq. (2.1) where SU(2) symmetry is restored by adding

a small staggered magnetic field

$$\mathcal{H}_{J_1-J_2} = J_1 \sum_{\langle ij \rangle} \vec{S}_i \cdot \vec{S}_j + J_2 \sum_{\langle\langle ij \rangle\rangle} \vec{S}_i \cdot \vec{S}_j + h^* \sum_i (-1)^i S_i^z, \quad (3.1)$$

such that $\langle S_i^z \rangle = 0$, as well as the ferromagnetic XY model

$$\mathcal{H}_{XY} = -J \sum_{\langle ij \rangle} (S_i^x S_j^x + S_i^y S_j^y) + h^* \sum_i S_i^x, \quad (3.2)$$

where the transverse field h^* is chosen such that $\langle S_i^x \rangle = 0$ and $\langle S_i^y \rangle = 0$ in order to artificially restore the U(1) symmetry. In both cases, the external field $h^* \propto L^{-4}$ leads to a finite size gap $\Delta \sim \sqrt{h^*} \sim 1/L^2$, below the n_G linearly dispersing Goldstone modes ($n_G = 2$ for the SU(2) $J_1 - J_2$ model, and $n_G = 1$ for the U(1) XY model). This additional energy scale reproduces the TOS structure on finite systems. For the analytical expressions below, we do not specify the value of the spin S , while for the numerical computations we explicitly consider $S = 1/2$.

The calculation of the EEs in the SW approximation is eased by the quadratic nature of the SW Hamiltonian (at the linear harmonic level), as the reduced density matrix can be expressed as an exponential of a correlation matrix C involving only expectation values of two-point correlation functions^{20,21}. The EEs of a subsystem composed of N_A sites are obtained as a function of the N_A eigenvalues ν_p^2 of this correlation matrix:

$$S_q = \frac{1}{q-1} \sum_p \ln \left[\left(\nu_p + \frac{1}{2} \right)^q - \left(\nu_p - \frac{1}{2} \right)^q \right], \quad (3.3)$$

and for $q = 1$:

$$S_1 = \sum_p \left[\left(\nu_p + \frac{1}{2} \right) \ln \left(\nu_p + \frac{1}{2} \right) - \left(\nu_p - \frac{1}{2} \right) \ln \left(\nu_p - \frac{1}{2} \right) \right]. \quad (3.4)$$

The eigenvalues ν_p^2 are typically obtained from numerical diagonalization of the matrix C , once its elements have been evaluated for the value h^* (which depends on system size and parameters such as J_2 or the spin value S). In the case of a line subsystem, the numerical diagonalization step can be circumvented by noticing that the translation invariance along the line implies that the matrix C is *circulant*²²: its eigenvalues are given by the Fourier transform of its first line. Plugging in all the expectation values and exploiting the convolution theorem, we obtain

$$\nu_p = \frac{1}{2L} \sqrt{\left(\sum_{k_y} \frac{A(p, k_y)}{\Omega(p, k_y)} \right)^2 - \left(\sum_{k_y} \frac{B(p, k_y)}{\Omega(p, k_y)} \right)^2}, \quad (3.5)$$

where $p = -\pi + \frac{2\pi}{L}(j-1)$ with $j \in [1, L]$, and the SW

excitation spectrum $\Omega(\mathbf{k}) = \sqrt{A(\mathbf{k})^2 - B(\mathbf{k})^2}$ is given by

$$\begin{aligned} A(k_x, k_y) &= 2SJ_2 \cos k_x \cos k_y + 2S(J_1 - J_2) + \frac{h^*}{2} \\ B(k_x, k_y) &= -SJ_1 [\cos k_x + \cos k_y] \end{aligned} \quad (3.6)$$

for the $J_1 - J_2$ model, while for the XY case

$$\begin{aligned} A(k_x, k_y) &= -S\frac{J}{4} [\cos k_x + \cos k_y] + SJ + \frac{h^*}{2} \\ B(k_x, k_y) &= S\frac{J}{4} [\cos k_x + \cos k_y]. \end{aligned} \quad (3.7)$$

The symmetry of the line subsystem allows to directly compute EEs within the SW approximation using Eq. (3.5) for systems of very large linear size (up to $L \sim 10^5$), which can hardly be reached if a numerical diagonalization of C is involved. Note that for such large systems, the regularizing field h^* becomes extremely small, and we resorted to arbitrary-precision numerics to ensure convergence of h^* and corresponding ν_p .

Considering now the case $S = 1/2$, our numerical results for S_q for different Rényi indices q are displayed in Fig. 3 (left) for the $J_1 - J_2$ Heisenberg model (for different values of the diagonal coupling J_2) and in Fig. 4 (left) for the XY model. The precise value of S_q being dominated by a non-universal area law term, one cannot directly compare the actual estimates of S_q obtained within SW to our exact QMC results at small sizes due to the approximations inherent to the SW approach. However, we expect the universal subleading logarithmic scaling term to be well captured by the modified SW theory. Indeed, fitting our SW data to the previous form Eq. (2.2) clearly yields an additive logarithmic term, as shown in Fig. 5 for the $J_1 - J_2$ antiferromagnet with $J_2 = -1$ and in Fig. 6

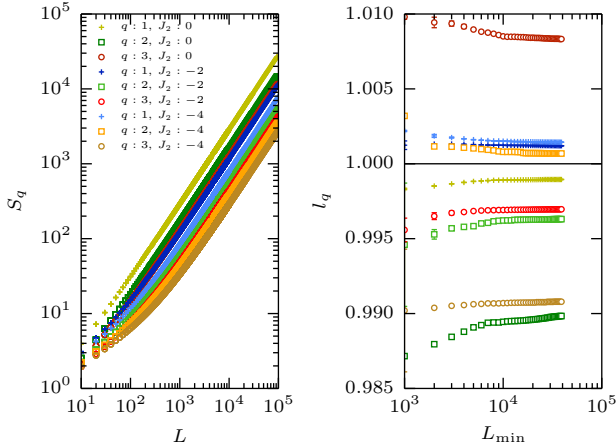


Figure 3. (Color online) Left panel: EE S_q of the line shaped subsystem in the $J_1 - J_2$ model for different values of J_2 and Rényi indices q as obtained from the modified spinwave analysis. Right panel: Prefactors l_q of the logarithmic corrections obtained from fits of the form $abl'l''c'$ (cf. Eq. (3.8) for definitions of the terms) as a function of the minimal size L_{\min} included in the fit.

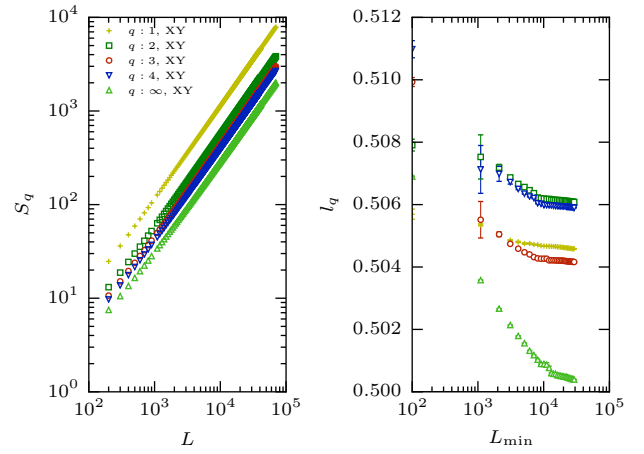


Figure 4. (Color online) Left panel: EE S_q of the line shaped subsystem in the XY model for different Rényi indices q . Right panel: Logarithmic term in the scaling of the EE of a line in the XY model for different fit ranges $[L_{\min}, 7 \cdot 10^4]$ and different Rényi indices q , as obtained from a fit of the form $abl'l''c'$ (see Eq. (3.8)).

for the XY model. The slow convergence of the coefficient of the logarithmic term suggests that subleading corrections beyond the log term in Eq. (2.2) have to be included. As we are not aware of any prediction for such subleading corrections, we perform fits using the general ansatz

$$\begin{aligned} S_q &= a_q L + l_q \ln L + b_q \\ &+ l_q^2 \ln \ln L + l_q^3 \ln \ln \ln L + \frac{c_q}{L} + c_q^1 \frac{\ln L}{L}, \end{aligned} \quad (3.8)$$

leaving out systematically various terms. We use the shorthand notation $abl^2l^3c^1c$ to label the various fit functions in the following figures (terms whose parameters do not appear in this string are not included in the fits). We find nonvanishing contributions for all terms and comparing carefully the distance of the fit to the data quantified by χ^2 , it seems that the inclusion of all these terms yields the best fits. We show a representative analysis of different fit functions in Fig. 5 for the $J_1 - J_2$ model and in Fig. 6 for the XY model. The comparison of the distances of the studied fit functions to the data shown in the right panels of Figs. 5 and 6 indicates that the most reliable description of the data is obtained by the ansatz $abl^2l^3c^1$, which seems reasonable as the term $c^1 \ln L/L$ decreases slowly and may therefore still be important at the available system sizes.

A word of caution is in order here regarding the meaning of χ^2 . This quantity is usually normalized by (gaussian) statistical errorbars attached to the data and should therefore follow the χ^2 distribution. In particular, this implies that χ^2/ndf for a perfect fit approaches unity and can not be smaller unless the model “overfits” statistical noise. Here, the situation is strikingly different as our data do not bear statistical errorbars and χ^2 does not

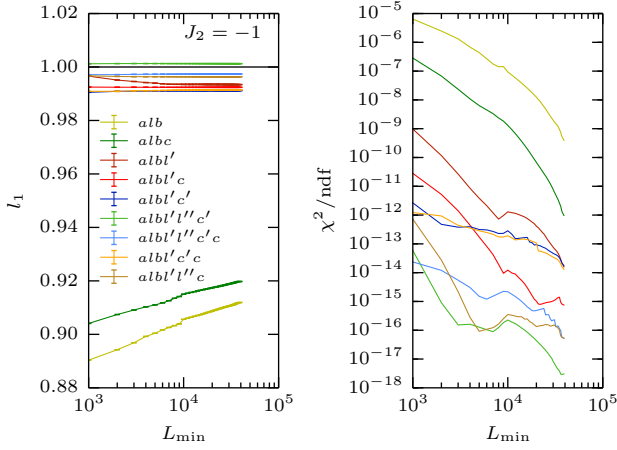


Figure 5. (Color online) Comparison of different fits over the range $[L_{\min}, 10^5]$ to the spin wave result for S_1 at $J_2 = -1$ in the $J_1 - J_2$ Heisenberg model. The left panel displays the prefactor l_1 of the logarithmic scaling term $l_1 \ln(L)$, which all fits find to be very close to unity. The right panel displays the corresponding χ^2 normalized by the number of degrees of freedom (ndf). Clearly the best fits with the lowest χ^2 find l_1 to be closest to 1. The artifacts around $L_{\min} \approx 10^4$ stem from a change of the grid on which we calculated S_1 which effectively introduces a higher weight for points in the denser region of the grid at smaller system size. The fit functions are coded according to the terms in equation (3.8).

have any statistical meaning. In fact, for a perfect fit, χ^2 would then vanish, a situation we are very close to. The slow growth of the different fitting terms as well as the fact that the exact form of the subleading terms in the scaling below the logarithmic term remain unknown still gives rise to a small uncertainty of our fit results.

Despite this, the different results for the investigated *ansätze* consistently yield a logarithmic prefactor which is very close to (or evolves with growing system sizes into) $l_q = 1$ for the $J_1 - J_2$ Heisenberg model and $l_q = 1/2$ for the XY model. This can be clearly seen in Figs. 5 and 6 for l_1 , and for l_q in Figs. 3 and 4 for different values of q (as well as different J_2 for the $J_1 - J_2$ Heisenberg model).

Our high-precision spin-wave results for a line subsystem are therefore in full agreement with the prediction Eq. (1.2) of a prefactor $l_q = n_G/2$ reflecting the number of Goldstone modes associated with the breaking of a continuous symmetry.

From the structure of the eigenvalues of the correlation matrix Eq. (3.5) one can go further to interpret the additive logarithmic term in terms of the number of Goldstone modes n_G . Indeed, one can rewrite them as

$$\nu_p = \frac{1}{2L} \sqrt{\sum_{k_y} \Theta(p, k_y) \sum_{k_y} \Theta^{-1}(p, k_y)}, \quad (3.9)$$

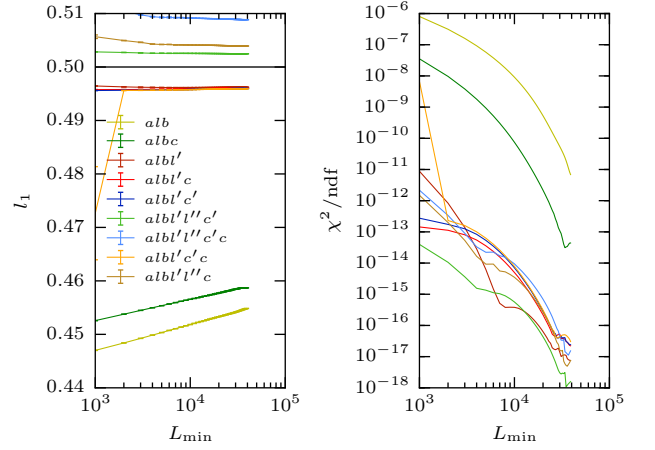


Figure 6. (Color online) Comparison of different fits over the range $[L_{\min}, 7 \cdot 10^4]$ to the spin wave result for S_1 in the XY model. The left panel displays the prefactor l_1 of the logarithmic scaling term $l_1 \ln(L)$, which all fits find to be very close to one half. The right panel displays the corresponding χ^2 normalized by the number of degrees of freedom (ndf). Clearly the best fits with the lowest χ^2 find l_1 to be closest to 0.5. The fit functions are coded according to the terms in equation (3.8).

with

$$\Theta(p, k_y) = \sqrt{\frac{A(p, k_y) - B(p, k_y)}{A(p, k_y) + B(p, k_y)}}, \quad (3.10)$$

A and B being given by Eqs. (3.6) and (3.7), and the L modes $p = -\pi + \frac{2\pi}{L}(j-1)$ with $j = 1, \dots, L$. It is straightforward to see that all Θ are non-singular $O(1)$ numbers, except at the singular points where Goldstone modes vanish. More precisely for $SU(2)$ there are two contributions

$$\Theta^{SU(2)}(0, 0) = \frac{1}{\Theta^{SU(2)}(\pi, \pi)} \simeq \sqrt{\frac{8SJ_1}{h^*}} \simeq 2Nm_{AF}, \quad (3.11)$$

where m_{AF} is the thermodynamic limit ($SU(2)$ broken) staggered magnetization, and one contribution for $U(1)$

$$\Theta^{U(1)}(0, 0) \simeq \sqrt{\frac{SJ}{h^*}} \simeq 4Nm_{xy}, \quad (3.12)$$

where m_{xy} is the transverse order in the thermodynamic limit. Therefore all eigenvalues ν_p are $O(1)$ away from the Goldstone points where instead

$$\nu_{\text{Goldstone}} \propto \sqrt{L} + \text{constant}. \quad (3.13)$$

Plugging this into the expression of the Rényi EEs Eq. (3.3), the $L - n_G$ modes with $O(1)$ eigenvalues will add up and contribute $\sim L$ (the area law part) to S_q and the n_G terms will each contribute $\frac{1}{2} \ln L$, $\forall q$.

IV. DISCUSSIONS AND CONCLUSIONS

We have investigated predictions from field theory that spontaneous breaking of a continuous symmetry leads to a logarithmic subleading scaling of the EEs S_q independent on microscopic parameters and the Rényi index q , in the specific case of a periodic line subsystem embedded in a two-dimensional torus. Our results, obtained using two different methods (numerically exact QMC and spin wave theory), are in perfect agreement with the prediction that the prefactor of the logarithmic term is given by $l_q = n_G/2$ by studying two models breaking SU(2) and U(1) symmetry respectively.

Interestingly, we find that it is not necessary to study a bipartition of the system in two equal parts as cutting out a one dimensional subsystem is sufficient to capture the universal logarithmic correction. This is beneficial for both methods used in this work and we believe that other numerical and analytical techniques can profit from this finding in order to push calculations to larger system sizes, which are of tremendous importance for fitting the logarithmic term. Moreover, the spin-wave theory of the entanglement entropy of a line subsystem allows simplified calculations where the contribution of each Goldstone mode can be fully understood analytically in the modified (symmetry restored) spin-wave theory formal-

ism.

Reaching very large system sizes allowed us to capture higher order finite size corrections which demonstrates that it is very difficult to get a precise and size-converged estimate for the prefactor of the logarithmic correction l_q using QMC simulations, restricted to linear sizes of a few tens of sites.

Beyond this case of continuous symmetry-breaking phases, it would be interesting to investigate whether the line subsystem can also capture subdominant universal corrections associated with other types of phases, such as discrete symmetry-breaking or topological phases. Indeed in the latter case, a one-dimensional geometry, as used in Ref. 23, appears computationally more tractable (especially within QMC) than the usual topological entanglement entropy constructions^{5,6,24}.

ACKNOWLEDGMENTS

It is our pleasure to thank G. Misguich and M. Oshikawa for inspiring discussions and collaborations on related topics. X.P. acknowledges Y. Fuji for interesting suggestions. This work was performed using HPC resources from GENCI (grant x2015050225) and CALMIP (grant 2015-P0677), and is supported by the French ANR program ANR-11-IS04-005-01. Our QMC simulations partly use the ALPS libraries²⁵.

-
- ¹ P. Calabrese, J. Cardy, and B. Doyon, *Journal of Physics A: Mathematical and Theoretical* **42**, 500301 (2009).
 - ² T. Grover, Y. Zhang, and A. Vishwanath, *New Journal of Physics* **15**, 025002 (2013).
 - ³ M. Srednicki, *Phys. Rev. Lett.* **71**, 666 (1993).
 - ⁴ J. Eisert, M. Cramer, and M. Plenio, *Rev. Mod. Phys.* **82**, 277 (2010).
 - ⁵ A. Kitaev and J. Preskill, *Phys. Rev. Lett.* **96**, 110404 (2006).
 - ⁶ M. Levin and X.-G. Wen, *Phys. Rev. Lett.* **96**, 110405 (2006).
 - ⁷ M. A. Metlitski and T. Grover, *arXiv:1112.5166* (2011).
 - ⁸ P. W. Anderson, *Phys. Rev.* **86**, 694 (1952).
 - ⁹ H. Song, N. Laflorencie, S. Rachel, and K. Le Hur, *Phys. Rev. B* **83**, 224410 (2011).
 - ¹⁰ A. B. Kallin, M. B. Hastings, R. G. Melko, and R. R. P. Singh, *Phys. Rev. B* **84**, 165134 (2011).
 - ¹¹ S. Humeniuk and T. Roscilde, *Phys. Rev. B* **86**, 235116 (2012).
 - ¹² J. Helmes and S. Wessel, *Phys. Rev. B* **89**, 245120 (2014).
 - ¹³ B. Kulchytskyy, C. M. Herdman, S. Inglis, and R. G. Melko, *arXiv:1502.01722* (2015).
 - ¹⁴ M. Takahashi, *Phys. Rev. B* **40**, 2494 (1989).
 - ¹⁵ J. E. Hirsch and S. Tang, *Phys. Rev. B* **40**, 4769 (1989).
 - ¹⁶ D. J. Luitz, X. Plat, N. Laflorencie, and F. Alet, *Phys. Rev. B* **90**, 125105 (2014).
 - ¹⁷ A. W. Sandvik and J. Kurkijärvi, *Phys. Rev. B* **43**, 5950 (1991).
 - ¹⁸ O. F. Syljuåsen and A. W. Sandvik, *Phys. Rev. E* **66**, 046701 (2002).
 - ¹⁹ A. P. Young, *arXiv:1210.3781* (2012).
 - ²⁰ M. B. Plenio, J. Eisert, J. Dreißig, and M. Cramer, *Phys. Rev. Lett.* **94**, 060503 (2005).
 - ²¹ T. Barthel, M.-C. Chung, and U. Schollwöck, *Phys. Rev. A* **74**, 022329 (2006).
 - ²² For the SU(2) case more precisely, the matrix C is block-diagonal with two identical circulant blocks (corresponding to correlations between odd and even sublattice sites of the bipartite lattice), and each block contributes half of the eigenvalues mentioned in Eq. (3.5).
 - ²³ S. Furukawa and G. Misguich, *Phys. Rev. B* **75**, 214407 (2007).
 - ²⁴ S. V. Isakov, M. B. Hastings, and R. G. Melko, *Nature Physics* **7**, 772 (2011).
 - ²⁵ B. Bauer, L. D. Carr, H. G. Evertz, A. Feiguin, J. Freire, S. Fuchs, L. Gamper, J. Gukelberger, E. Gull, S. Guertler, A. Hehn, R. Igarashi, S. V. Isakov, D. Koop, P. N. Ma, P. Mates, H. Matsuo, O. Parcollet, G. Pawłowski, J. D. Picon, L. Pollet, E. Santos, V. W. Scarola, U. Schollwöck, C. Silva, B. Surer, S. Todo, S. Trebst, M. Troyer, M. L. Wall, P. Werner, and S. Wessel, *Journal of Statistical Mechanics: Theory and Experiment* **2011**, P05001 (2011).